Distal Effect of Amide and Amino Groups on the Oxygen Activation Ability and Rate of the Redox Reaction of Simplified Analogs of Bleomycin

Takayuki Arai, Kazuo Shinozuka, and Hiroaki Sawai*

Department of Chemistry, Faculty of Engineering, Gunma University, Kiryu, Gunma 376

(Received November 18, 1997)

New simple bleomycin (BLM) model compounds, which bear a carbamide (**1**), bulky *t*-butyl (**2**), simple alkyl (**3**), or amino group (**4**) around the sixth coordination site, have been synthesized in order to study the effect of the distal substituents on the redox reaction and oxygen activation ability of the iron complexes. The carbamide group in **1** lowers the p*K* values of the all-amino donors of the ligand, which enhances complex formation. The oxygen activation ability of the Fe(II) complexes of **1**, **2**, **3**, and **4**, is 74, 69, 43, and 41%, respectively, of that of BLM. The rate of reduction of the Fe(III) complexes of the model compounds and BLM with a reducing agent is more than ten-times lower than that of the oxygenation and activation of the corresponding Fe(II) complexes, indicating the low turnover of the iron complexes of the model compounds and BLM in the reversible redox reaction.

Bleomycin (BLM), used in cancer chemotherapy, is a glycopeptide isolated from cultures of *Streptomyces verticillus* as a Cu(II) complex.[1,2] The therapeutic effect of BLM is thought to be yielded by the cleavage of cellular DNA, which occurs in the presence of Fe(II) and oxygen.[3—8] Oxygenation, followed by the oxidation of the Fe(II) complex of BLM, results in the formation of activated oxygen.[4—13] The resulting Fe(III) complex of BLM is reduced to the orignal BLM–Fe(II) complex with a reducing agent to attain the cycle of the redox reaction. The oxidative cleavage of DNA by the iron complex of BLM has attracted special attention because Fe–BLM comprises the first example of non-heme iron complexes with significant dioxygen activation.[14] The BLM is commonly divided into three functional subunits: a bithiazole moiety, which facilitates DNA binding; a pseudopeptide portion, which acts as a metal chelating domain; and a disaccharide moiety. The metal chelating domain is considered to be the crucial portion of BLM. A number of simplified synthetic analogs of BLM have been synthesized in order to study the functional roles of the individual subunits.[15—42] Among the BLM subunits, the role of the disaccharide moiety including the carbamoyl group is most poorly understood, although the disaccharide moiety is thought to control the uptake of BLM by cells and to stabilize the reactive oxygenated BLM–iron species by forming a protecting pocket in the surrounding coordination sphere.[15,43,44] The carbamoyl group on the terminal carbohydrate of BLM has been suspected to coordinate to the Fe(II) ion as a sixth ligand.[45—47] The appropriate BLM model compounds will provide insight into the role of the carbamoyl group of BLM, a putative sixth ligand for metal complexing (Fig. 1). For decarbamoyl-BLM, a derivative that differs from natural BLM only by the absence of a carbamoyl group in mannose, although the efficiency and specificity of DNA cleavage is similar to that of natural BLM, a significant difference in cleavage-site specificity was observed between the decarbamoyl and original BLMs.[45—47] This has been attributed to the role of the carbamoyl group in the determination of the metal coordination geometry. On the other hand, Boger et al. recently claimed that the carbamoyl group on mannose has little effect on the DNA cleavage, oxygen activation and metal complexation based on comparative studies of the DNA cleavage by BLM and decarbamoyl BLM.[48] They have concluded that although the first monossaccharide is sufficient for the activity of BLM, the role of the carbamoyl group is very subtle.[48] Thus, there has been some discrepancy regarding the role of the carbamoyl group in BLM for metal complexation, oxygen activation, and DNA cleavage. Very recently, we have reported on the preparation of a simple BLM model compound bearing a carbamide group around the sixth coordination site, which may coordinate to the chelated iron as a sixth ligand (**1**).[49] This iron complex exhibited high oxygen-activation ability. The result suggests that the ligation group around the sixth coordination site has a profound effect on the redox reaction of BLM and its model compounds. Further, we have synthesized several BLM model compounds with or without a terminal group (**2**—**4**) which can or cannot coordinate to the iron ion as a sixth ligand, and examined their properties in detail along with those of **1** and a model compound with no substituent group (**5**).[50] We have especially studied oxygen activation ability, the reaction rates of the oxygenation and the reduction of the iron–BLM model compounds along with those of BLM in order to gain information on the role of the carbamoyl group in the redox reaction of iron–BLM or model complexes.

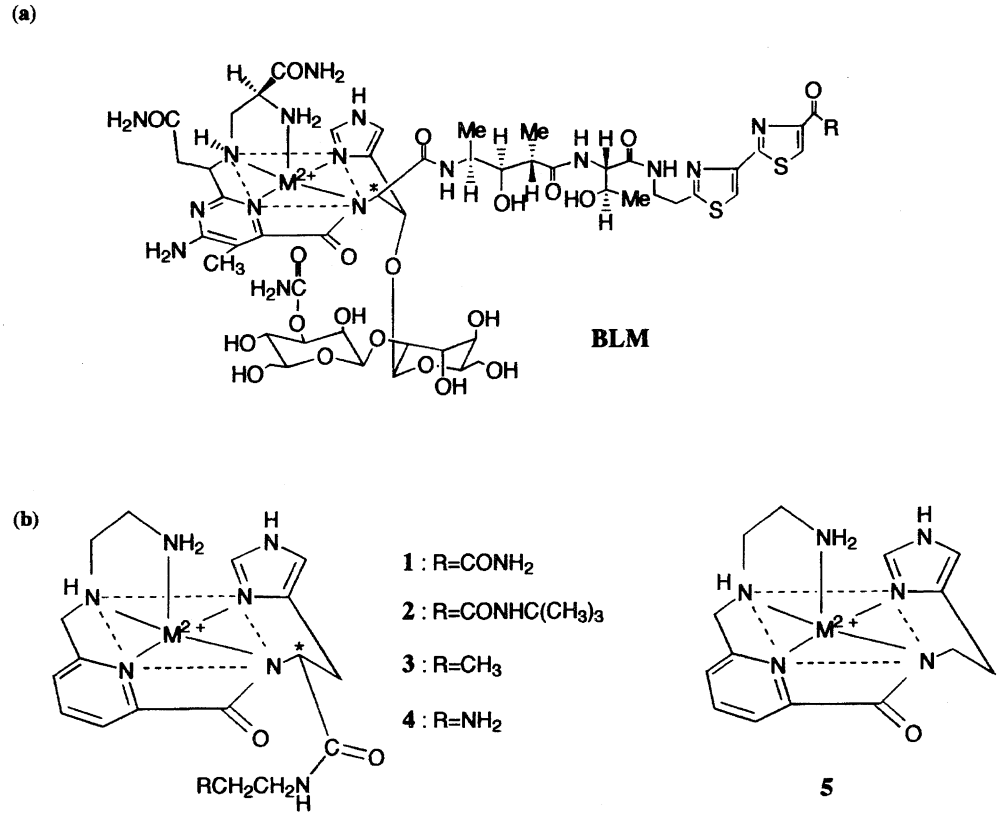

Fig. 1. BLM (a) and BLM model complexes (b).

Experimental

General Methods. All of the materials obtained commercially were used without further purification. The melting points were determined by using a Yanaco micro-melting-point apparatus (MP 500D). ^{1}H NMR spectra were obtained on a Varian Gemini 200 FT-NMR using sodium 3(trimethylsilyl)-1-propanesulfonate in D_2O and tetramethylsilane (Me_4Si) in $CDCl_3$ or CD_3OD, or $(CD_3)_2SO$ as internal references. IR spectra were taken on a Hitachi 270-50. Mass spectra (ES-MS) were obtained on a Perkin–Elmer Sciex API-100 electrospray mass spectrometer with a positive mode. UV-visible spectra were recorded on a Hitachi U-3200. EPR spectra, both at 25 °C and 77 K, were recorded with a JEOL JES-RE2X spectrometer operating with 100 kHz magnetic field modulation using Mn^{II}-doped MgO powder as a reference ($g_3 = 2.034$ and $g_4 = 1.981$). Stopped-flow measurements were carried out using an Otsuka Electronics RA401.

Synthesis of Model Compounds of BLM, 1—4. Methyl 6-({*N*-[2-(Benzyloxycarbonylamino)ethyl]-*N*-benzyloxycarbonylamino}methyl)pyridine-2-carboxylate (7). Methyl 6-formylpyridine 2-carboxylate (**6**) was prepared according to the procedure of Mathes et al.[51] with a slight modification. A solution of **6** (1.85 g, 11.2 mmol) and [2-(*N*-benzyloxycarbonylamino)ethyl]amine (2.63 g, 13.5 mmol) in 75 ml of CH_3CN was stirred at room temperature in the presence of an activated molecular sieve (4 Å) under Ar overnight. The mixture was concentrated to dryness in vacuo. The residue was dissolved in MeOH (75 ml) and $NaBH_4$ (510 mg, 13.5 mmol) was added to the solution. After being stirred for 2 h at room temperature, the solution was adjusted to pH 7.0 with 0.5 M-aqueous tartaric acid (1 M = 1 mol dm^{-3}), filtrated through Celite and concentrated under reduced pressure. To the solution of the residue in CH_2Cl_2 (50 ml) and 0.2 M-NaOH (84 ml) was added dropwise benzyloxycarbonyl chloride (2.37 ml, 16.6 mmol) in 10 ml of CH_2Cl_2. The mixture was stirred for 3 h at room temperature, and the aqueous layer was extracted five times with CH_2Cl_2. The CH_2Cl_2 layers were combined and dried over $MgSO_4$. The residue was purified by chromatography on silica gel (eluted with CH_2Cl_2 : ethyl acetate = 1 : 1) to give a colorless oil. Recrystallization of the residue from 2-propanol afforded **7** (4.86 g, 91% yield) as a white crystalline solid. Mp 86.2—86.6 °C; ^{1}H NMR ($CDCl_3$) $\delta = 3.42$ (t, 2H, $J = 6.0$ Hz, NCH_2), 3.65 (t, 2H, $J = 6.0$ Hz, CH_2NH), 3.85 (s, 3H, OCH_3), 4.75 (s, 2H, $PyCH_2$) 4.98—5.12 (m, 4H, each $PhCH_2$), 7.30 (s, 5H, Ph), 7.31 (s, 5H, Ph), 7.68 [t, 1H, $J = 6.0$ Hz, Py (5)], 7.81 [t, 1H, $J = 6.0$ Hz, Py (4)], 8.01 [t, 1H, $J = 6.0$ Hz, Py (3)]; IR (KBr) 1723 s, 1712 s, 1509 m, 1263 s, 1138 m, 1005 m, 800 m cm^{-1}. ES-MS Found: *m/z* 478.6. Calcd for $C_{26}H_{28}N_3O_6$: $(M+H)^+$, 478.2.

Methyl N^{α}-[6-({*N*-[2-(Benzyloxycarbonylamino)ethyl]-*N*-benzyloxycarbonylamino}methyl)-2-pyridylcarbonyl]-L-histidinate (8). A 0.1 M LiOH solution (15 ml) was added to a solution of **7** (480 mg, 1.01 mmol) in THF (8 ml) at 0 °C. After the solution was stirred at 0 °C for 2 h water (15 ml) was added and the resulting solution was concentrated in vacuo. The residue was adjusted to pH 3 with 10%-aqueous citric acid and extracted five times with CH_2Cl_2. The CH_2Cl_2 layers were combined and dried over $MgSO_4$ and evaporated in vacuo. The residue and L-Histidine methyl ester dihydrochloride (362 mg, 1.50 mmol) were dissolved in DMF (3 ml) under N_2. Diphenylphosphoryl azide (DPPA; 323 µl, 1.50 mmol) in DMF (3 ml) was successively added to the solution at 0 °C; after being stirred at 0 °C for 10 min, Et_3N (627 µl, 4.50 mmol) in DMF (3 ml) was added to the solution at 0 °C. After being stirred at 0 °C for 3 h, then at room temperature for 3 d, the

solution was concentrated in vacuo. The residue was purified by chromatography on silica gel (eluted with CH_2Cl_2 : MeOH = 13 : 2) to give **8** as a colorless oil (615 mg, quantitative). ^{1}H NMR ($CDCl_3$) δ = 3.22—3.43 (m, 4H, each CH_2 of ethylenediamine), 3.48 (t, 2H, J = 6.0 Hz, C$_\alpha H_2$ of His), 3.74 (s, 3H, OCH_3), 4.71 (s, 2H, PyCH_2), 4.98 (t, 1H, J = 10 Hz, CH), 5.05—5.15 (m, 4H, each PhCH_2), 7.33—7.40 (m, 12H, each Ph and Im), 7.52 [d, 1H, J = 6.0 Hz, Py (5)], 7.89 [d, 1H, J = 6.0 Hz, Py (4)], 8.06 [t, 1H, J = 6.0 Hz, Py (3)]. ES-MS Found: m/z 615.2. Calcd for $C_{32}H_{35}N_6O_7$: $(M+H)^+$, 615.2.

3-{N^α-[6-({N-[2-(Benzyloxycarbonylamino)ethyl]-N-(benzyloxycarbonyl)amino}methyl)-2-pyridylcarbonyl]-L-histidinylamino}propionamide (9). A 0.1 M LiOH (15 ml) was added to a solution of ester **8** (580 mg, 944 mmol) in THF (5 ml) at 0 °C. After the solution was stirred at 0 °C for 2 h, water (7.5 ml) was added and the resulting solution was concentrated in vacuo. The residue was adjusted to pH 3 with 10%-aqueous citric acid and extracted with CH_2Cl_2 five times. The CH_2Cl_2 layers were combined and dried over $MgSO_4$ and evaporated in vacuo. The residue and 3-aminopropionamide (119 mg, 1.35 mmol) were dissolved in DMF (3 ml) under N_2. DPPA (291 µl, 1.35 mmol) in DMF (3 ml) was successively added to the solution at 0 °C, and after being stirred at 0 °C for 20 min, Et_3N (188 µl, 1.35 mmol) in DMF (3 ml) was added to the solution at 0 °C. After being stirred at 0 °C for 3 h, and then at room temperature for 2 d, the solution was concentrated in vacuo. Ethyl acetate (200 ml) was added to the residue and washed with 5%-aqueous $NaHCO_3$ (20 ml). Filtration of the resulting insoluble white crystal gave **9** (530 mg, 84% yield). Mp 167.6—168.5 °C; ^{1}H NMR [$(CD_3)_2SO$] δ = 2.18 (t, 2H, J = 7.0 Hz, C$_\beta H_2$ of β-Ala), 2.93—2.98 (m, 2H, C$_\alpha H_2$ of β-Ala), 3.17—3.33 (m, 4H, each CH_2 of ethylenediamine), 3.43—3.52 (m, 4H, C$_\alpha H_2$ of His), 4.53—4.68 (m, 3H, PyCH_2 and CH), 4.97—5.12 (m, 4H, each PhCH_2), 6.83 [s, 1H, Im (5)], 7.22—7.45 [m, 11H, each Ph and Py (5)], 7.53 [s, 1H, Im (2)], 7.88—7.96 [m, 2H, Py (3, 4)]; IR (KBr) 3296 s (br), 1700 s, 1686 s, 1672 s, 1653 s, 1559 m, 1543 m, 1262 s (br) cm^{-1}. ES-MS Found: m/z 671.0. Calcd for $C_{34}H_{39}N_8O_7$: $(M+H)^+$, 671.3.

3-(N^α-{6-[(2-Aminoethyl)aminomethyl]-2-pyridylcarbonyl}-L-histidinylamino)propionamide (1). Bis-Z derivative **9** (160 mg, 239 µmol) in the solution (10 ml, MeOH : H_2O : HCOOH = 70 : 29 : 1) was hydrogenated in the presence of Pd–carbon (24 mg) under atmospheric pressure of H_2 at 0 °C. The solution was allowed to gradually warm to room temperature, and then stirred for 3 h at the same temperature. After the filtration of Pd–carbon through Celite, the filtrate was concentrated in vacuo. The residue was purified by chromatography on silica gel (eluted with CH_2Cl_2 : MeOH : 25% aqueous NH_3 = 16 : 4 : 1) to give **1** as a white powder (96 mg, quantitative). Mp 146.0—148.3 °C; $[\alpha]_D^{20}$ +5.6 (c 0.25, MeOH : H_2O = 4 : 1); ^{1}H NMR (D_2O) δ = 2.48 (t, 2H, J = 5.7 Hz, C$_\beta H_2$ of β-Ala), 2.75—2.85 (m, 4H, each CH_2 of ethylenediamine), 3.23 (d, 2H, J = 6.1 Hz, C$_\alpha H_2$ of His), 3.46—3.51 (m, 2H, C$_\alpha H_2$ of β-Ala), 4.00 (s, 2H, PyCH_2), 4.79 (t, 1H, J = 7.2 Hz, CH), 7.03 [s, 1H, Im (5)], 7.58 [d, 1H, J = 7.0 Hz, Py (5)], 7.74 [s, 1H, Im (2)], 7.86—8.00 [m, 2H, Py (3, 4)]: IR (KBr) 3295 s (br), 1674 s, 1651 s, 1645 s, 1538 m, 1456 m cm^{-1}. ES-MS Found: m/z 403.4. Calcd for $C_{18}H_{27}N_8O_3$: $(M+H)^+$, 403.2.

1 (96 mg, 0.23 mmol) was poured into a solution of 60%-$HClO_4$ (77 µl, 0.29 mmol) in EtOH (5 ml) and recrystallized from 2-propanol/MeOH (1 : 1) to obtain **1**·3$HClO_4$ salt (157 mg) as a white solid. Found: C, 30.67; H, 4.52; N, 15.01%. Calcd for $C_{18}H_{29}Cl_3N_8O_{15}$·3$H_2O$·1/2$CH_3OH$: C, 30.64; H, 4.61; N, 15.04%.

3-{N^α-[6-({N-[2-(Benzyloxycarbonylamino)ethyl]-N-(benzyloxycarbonyl)amino}methyl)-2-pyridylcarbonyl]-L-histidinylamino}N-t-butylpropionamide (10). Compound **10** was prepared from **8** (612 mg, 996 µmol) and 3-amino-N-t-butylpropionamide (196 mg, 1.36 mmol) as described above as a white powder (602 mg, 83% yield). Mp 86.5—87.1 °C; ^{1}H NMR ($CDCl_3$) δ = 1.27 (s, 9H, C(CH_3)$_3$), 2.16—2.38 (m, 2H, C$_\beta H_2$ of β-Ala), 3.10—3.20 (m, 2H, C$_\alpha H_2$ of β-Ala), 3.33—3.58 (m, 6H, each CH_2 of ethylenediamine and C$_\alpha H_2$ of His), 4.62 (s, 2H, PyCH_2), 4.83 (t, 1H, J = 5.0 Hz, CH), 5.04—5.16 (m, 4H, each PhCH_2), 6.78 [s, 1H, Im (5)], 7.22—7.47 [m, 11H, each Ph and Im (2)], 7.50 [d, 1H, J = 14 Hz, Py (5)], 7.67—7.82 [m, 1H, Py (4)], 8.02 [d, 1H, J = 6.0 Hz, Py (3)]; IR (KBr) 3418 (br), 1684 m, 1652 s, 1520 m, 1456 m, 1234 s (br) cm^{-1}. ES-MS Found: m/z 727.0. Calcd for $C_{38}H_{47}N_8O_7$: $(M+H)^+$, 727.3.

3-(N^α-{6-[(2-Aminoethyl)aminomethyl]-2-pyridylcarbonyl}-L-histidinylamino)-N-t-butylpropionamide (2). Bis-Z derivative **10** (600 mg, 825 µmol) was hydrogenated in the presence of Pd–carbon (108 mg) and purified as described above to give **2** as a white powder (376 mg, 99% yield). Mp 126.0—128.8 °C; $[\alpha]_D^{20}$ +10.4 (c 0.25, MeOH); ^{1}H NMR (D_2O) δ = 1.24 (s, 9H, C(CH_3)$_3$), 2.37 (t, 2H, J = 7.0 Hz, C$_\beta H_2$ of β-Ala), 2.82—3.03 (m, 4H, each CH_2 of ethylenediamine), 3.23 (d, 2H, J = 4.0 Hz, C$_\alpha H_2$ of β-Ala), 3.48 (t, 2H, J = 6.0 Hz, C$_\beta H_2$ of His), 4.00 (s, 2H, PyCH_2), 4.83 (t, 1H, J = 7.0 Hz, CH), 7.04 [s, 1H, Im (5)], 7.60 [d, 1H, J = 7.2 Hz, Py (5)], 7.71 [s, 1H, Im (2)], 7.90—8.02 [m, 2H, Py (3, 4)]; IR (KBr) 3421 s (br), 2921 w, 1653 s, 1646 m, 1540 m, 1522 m, 1323 m cm^{-1}. ES-MS Found: m/z 458.0. Calcd for $C_{22}H_{34}N_8O_3$: M^+, 458.3.

A perchlorate salt of **2** (65 mg, 0.14 mmol), synthesized as described above, was recrystallized from 2-propanol to obtain **2**·3$HClO_4$ salts (90 mg) as a white solid. Found: C, 33.65; H, 5.20; N, 12.90%. Calcd for $C_{22}H_{37}Cl_3N_8O_{15}$·3$H_2O$·1/2$(CH_3)_2CHOH$: C, 33.44; H, 5.63; N, 13.28%.

N^α-[6-({N-[2-(Benzyloxycarbonylamino)ethyl]-N-(benzyloxycarbonyl)amino}methyl)-2-pyridylcarbonyl-N-propyl]-L-histidinamide (11). Compound **11** was prepared from **8** (552 mg, 898 µmol) and 1-propylamine (111 µl, 1.35 mmol) as described above to give **11** as a while powder (334 mg, 57% yield). Mp 150.5—151.2 °C; ^{1}H NMR ($CDCl_3$) δ = 0.85 (t, 3H, J = 7.1 Hz, CH_3), 1.36—1.56 (m, 2H, CH_2CH$_3$), 1.73 (br, 1H, NH), 3.11—3.22 (m, 2H, CH_2CH_2CH$_3$), 3.31—3.56 (m, 6H, each CH_2 of ethylenediamine and C$_\alpha H_2$ of His), 4.56 (s, 2H, PyCH_2), 4.83 (t, 1H, J = 5.0 Hz, CH), 5.07—5.15 (m, 4H, each PhCH_2), 6.91 [s, 1H, Im (5)], 7.22—7.40 [m, 11H, each Ph and Im (2)], 7.54 [d, 1H, J = 14 Hz, Py (5)], 7.68—7.75 [m, 1H, Py (4)], 8.05 [d, 1H, J = 8.0 Hz, Py (3)]; IR (KBr) 3307 s, 1717 s, 1686 s, 1559 s, 1524 s, 1457 s, 1438 s (br) cm^{-1}. ES-MS Found: m/z 642.0. Calcd for $C_{34}H_{40}N_7O_6$: $(M+H)^+$, 642.3.

N^α-{6-[(2-Aminoethyl)aminomethyl]-2-pyridylcarbonyl}-N-propyl-L-histidinamide (3). Bis-Z derivative **11** (60 mg, 94 µmol) was hydrogenated in the presence of Pd–carbon (10 mg) and purified as described above to give **3** as a white powder (35 mg, quantitative). Mp 126.1—126.8 °C; $[\alpha]_D^{20}$ +11.9 (c 0.25, MeOH); ^{1}H NMR (D_2O) δ = 0.83 (t, 3H, J = 7.0 Hz, CH_3), 1.46 (t, 2H, J = 7.0 Hz, CH_2CH$_3$), 2.73—2.85 (m, 4H, each CH_2 of ethylenediamine), 3.05—3.31 (m, 4H, CH_2CH_2CH$_3$ and C$_\alpha H_2$ of His), 4.00 (s, 2H, PyCH_2), 4.78 (t, 1H, J = 6.3 Hz, CH), 7.02 [s, 1H, Im (5)], 7.56 [d, 1H, J = 8.0 Hz, Py (5)], 7.73 [s, 1H, Im (2)], 7.88—8.02 [m, 2H, Py (3, 4)]; IR (KBr) 3366 s, (br), 1653 s, 1644 s, 1560 m, 1542 m, 1458 m cm^{-1}. ES-MS Found: m/z 373.2. Calcd for $C_{18}H_{27}N_7O_2$: M^+, 373.5.

Perchlorate salt of **3** (93 mg, 249 µmol) was prepared as described above and recrystallized from 2-propanol to obtain the **3**·3$HClO_4$

salts (130 mg) as a yellow solid. Found: C, 32.04; H, 4.48; N, 14.53%. Calcd for $C_{18}H_{30}Cl_3N_7O_{14}$: C, 32.33; H, 4.60; N, 14.29%.

N^{α}[6-({*N*-[2-(Benzyloxycarbonylamino)ethyl]-*N*-{benzyloxycarbonylamino}methyl)-2-pyridylcarbonyl]-*N*-[2-(benzyloxycarbonylamino)ethyl]-L-histidinamide (12). Compound **12** was prepared from **8** (250 mg, 416 μmol) and [2-(*N*-benzyloxycarbonylamino)ethyl]amine (114 mg, 585 μmol) as described above to give **12** as a white powder (233 mg, 72% yield). Mp 114.2—115.6 °C; ^{1}H NMR ($CDCl_3$) δ = 3.08—3.45 (m, 8H, each CH_2 of ethylenediamine), 3.45—3.60 (m, 2H, $C_{\alpha}H_2$ of His), 4.60 (s, 2H, PyCH_2), 4.84—5.15 (m, 7H, each PhCH_2 and CH), 6.88 [s, 1H, Im (5)], 7.19—7.33 (m, 15H, each Ph), 7.35 [s,1H, Im (2)], 7.46 [d, 1H, J = 8.0 Hz, Py (5)], 7.62—7.75 [m, 1H, Py (4)], 7.99 [m, 1H, Py (3)]; IR (KBr) 3424 s (br), 1701 m, 1684 s, 1654 s, 1560 m, 1542 m, 1524 m, 1125 m, 670 m cm^{-1}. ES-MS Found: *m/z* 777.0. Calcd for $C_{41}H_{45}N_8O_8$: $(M+H)^+$, 777.3.

N^{α}-{6-[(2-Aminoethyl)aminomethyl]-2-pyridylcarbonyl}-*N*-(2-aminoethyl)-L-histidinamide (4). Bis-Z derivative **12** (233 mg, 300 μmol) was hydrogenated in the presence of Pd–carbon (25 mg) and purified as described above to give **4** as solid form (112 mg, quantitative). Mp 77.9—79.4 °C; $[\alpha]_D^{20}$ +18.0 (*c* 0.25, MeOH); ^{1}H NMR (D_2O) δ = 2.45—2.71 (m, 6H, CH_2 of ethylenediamine), 3.08—3.18 (m, 4H, $C_{\alpha}H_2$ of His and CONHCH_2CH_2), 3.81 (s, 2H, PyCH_2), 4.62 (t, 1H, J = 6.8 Hz, CH), 6.88 [s, 1H, Im (5)], 7.45 [dd, 1H, J = 1.2, 7.2 Hz, Py (5)], 7.58 [s, 1H, Im (5)], 7.73—7.85 [m, 2H, Py (3, 4)]; IR (KBr) 3420 s (br), 1700 m, 1684 s, 1653 s, 1637 m, 1560 m, 1542 m, 1523 m, 670 m cm^{-1}. ES-MS Found: *m/z* 374.1. Calcd for $C_{17}H_{26}N_8O_2$: M^+, 374.2.

Titration of the Ligands. Potentiometric titrations were carried out using a Fisher Accumet pH meter 15. All titration solutions were saturated with argon by passing a fine stream of argon bubbles through them for at least 1 h before titration; pH titration was carried out at 25.0 °C and I = 0.10 ($NaClO_4$) under argon. The titration point was obtained from a separately prepared solution to which was added the desired quantity of a 0.10 M NaOH solution. A calculation of the stability constants was carried out using the program SUPERQUAD developed by Gans et al.[52]

Preparation and Spectroscopic Studies of Iron Complexes of BLM Model Compounds. Iron Complexes. In a UV-visible spectra study, a solution of the Fe(II) complex (0.5 mM) in 50 mM Tris-HCl buffer (pH 7.2) was prepared by the addition of a stoichiometric amount of aqueous solution of $FeSO_4$ to a buffered solution of the model ligand under a stream of Ar. All solutions were purged of oxygen by swirling them for 2 h under a stream of Ar. A solution of the Fe(III) complex (0.5 mM) was prepared by bubbling oxygen into a solution of the Fe(II) complex. A DTT (dithiothreitol) adduct of the Fe(III) complex (0.5 mM) was prepared by the addition of a 2.0 mol equivalent of DTT (100 mM aqueous solution) to the Fe(III) complex. In an EPR study, a solution of a 2.0 mM Fe complex was obtained as described above, transferred to an EPR sample tube, and frozen in liquid nitrogen (77 K) immediately. In an IR study, a Fe(II) complex was prepared by mixing the model ligand with 1.2 mol equivalent of an oxygen-free aqueous solution of $FeSO_4$ (50 mM) under a stream of Ar. Oxygen-free acetone was added to the solution, and the supernatant was removed. The resulting deep-red precipitate was dried up in vacuo and suspended in nujol. The IR spectrum was recorded immediately.

Spin Trapping Experiment. The production of oxygenated free radicals during the formation of the Fe(III) complex from the Fe(II) complex (3.0 mM) was followed by the spin-trapping technique. An ethanolic solution of *N*-benzylidene-*t*-butylamine-*N*-oxide (*N*-*t*-butyl-α-phenylnitron, PBN) spin-trap agent (1.0 M, 150 μl) was added to a buffered solution (350 μl) of the Fe(II) complex. A solution of the Fe(II) complex was prepared by mixing an oxygen-free solution of $FeSO_4$ in water (20 mM, 50 μl) with an oxygen-free solution containing a 1.5 mol equivalent of the model ligand (10 mM, 150 μl), and the pH was adjusted to 7.2 with Tris-HCl buffer (1 M, 150 μl). After oxygen had been bubbled through the mixture for 15 s, an aliquot of the sample solution was rapidly transferred to a quartz cell for EPR measurements at 25 °C.

Kinetic Studies of Redox Reaction of the Iron Complex of the Model Compound. Oxidation of the Fe(II)-Complex. A stopped-flow kinetic measurement of the oxygenation of the Fe(II)-complex was made after rapidly mixing equal volumes of solutions of the Fe(II)–BLM-model complex and 0—2.0 mM oxygen. All of the solutions used in the experiments were purged of oxygen by swirling them for 2 h under a stream of N_2. A solution of Fe(II) complex (0.10 mM) in 10 mM Tris-HCl buffer was prepared by mixing an oxygen-free solution of iron(II) sulfate (0.10 mM) in water with oxygen-free solutions containing a 1.5 mol equivalent of the model compound, and the pH was adjusted to 7.2 by adding 1.0 M Tris-HCl (pH 7.2). Kinetic measurements were carried out using Otsuka electronics RA401 stopped-flow apparatus at 20 °C. The reaction of the Fe(II) complex with O_2 was monitored at the λ_{max} of the Fe(III) complex (384—391 nm), depending on each Fe(III) complex. The first rapid process was analyzed based on the spectral change between 50—120 ms after mixing, and the second slow process, at between 400—2100 ms when 2.0 mM–O_2 was used. The pseudo-first-order rate constant (k) was determined by Guggenheim equation,

$$kt + \ln(\lambda - \lambda_1) = \ln[(\lambda_0 - \lambda_\infty)\{1 - \exp(-k\Delta)\}]. \quad (1)$$

In Eq. 1, λ, λ_1, λ_0, and λ_∞ are the absorbance at t, $t+\Delta$, initial (t=0), and the final time after mixing, respectively, and Δ is an interval for the measurement of the absorbance. A plot of the pseudo-first-order rate constant against the O_2 concentration was linear, and the rate of the first step (k_{add}) was determined from the slope. The second kinetic event was first order with respect to the first accumulated product and independent of the oxygen concentration; therefore, the rate of the second step (k_{oxi}) coincides with the first-order rate constant.

Reduction of the Fe(III) Complex with DTT. The reduction process of the Fe(III) complex with DTT was monitored based on the UV-visible spectral change using a Hitachi UV 3200 double-beam spectrophotometer at 25 °C. The rates of the reactions were determined by monitoring the absorbance at 613 nm, which corresponds to the absorbance of the DTT adduct of the Fe(III) complex. The DTT–Fe(III) complex (0.5 mM) was prepared by the addition of 2.0 mol equivalent of DTT (aqueous solution) to the Fe(III)–BLM model complex in 50 mM Tris-HCl buffer (pH 7.2). The first step is the second-order reaction, and the rate constant (k_{add}) was determined by

$$1/(a-b)\cdot\ln[b(a-x)/a(b-x)] = k_{add}t. \quad (2)$$

In Eq. 2, k_{add} is the second-order rate constant for adduct formation and a and b are the initial concentration of the Fe(III) complex and DTT. x is the concentration of the DTT adduct of the Fe(III) complex after mixing t s. The rate constant of the second reaction (k_{red}) was determined by a Guggenheim plot (Eq. 1).

The first process was analyzed based on the spectral change between 0—1 min after mixing the solutions, and the second process was analyzed between 1—20 min after mixing when the Fe(III) complex of **1** was used.

Results and Discussion

We have recently shown that an iron complex of a simple BLM model compound bearing an alkyl tagged carbamide group, **1**, showed high oxygen activating ability.[49] To obtain information about the role of the carbamide group on the redox reaction of the iron complex, we have prepared and examined several BLM model compounds which have a carbamide (**1**), a bulky *t*-butylcarbamoyl (**2**), a simple alkyl (**3**), and a terminal amino (**4**) groups around the sixth coordination site. We also synthesized a simpler model compound bearing no substituent group (**5**) which was reported by Kimura et al.,[50] and compared its properties with those of the four model compounds, **1**—**4**. We conducted the synthesis of compounds by modifying a published procedure of Ohno et al.[16,29] and Lown et al.,[36] as depicted in Scheme 1. Aldehyde (**6**)[51] prepared from 2,6-pyridinedicarboxylic acid was condensed with [2-(*N*-benzyloxycarbonylamino)ethyl]-amine, followed by a reduction with sodium borohydride. A subsequent protection of the amino group with benzyloxycarbonyl chloride gave **7**. Compound **7** was hydrolyzed to the free acid and coupled with L-histidine methyl ester using diphenylphosphoryl azide as a condensing agent to afford compound **8** quantitatively. Saponification of the methyl ester of **8**, followed by coupling with β-alaninamide, *N*-*t*-butyl-β-alaninamide, propylamine, or the [2-(*N*-benzyloxycarbonylamino)ethyl]amine with diphenylphosphoryl azide, gave protected model compounds in 79, 83, 57, and 72% yield, respectively. A final removal of the benzyloxycabonyl group of the compounds was performed by hydrogenation on the Pd–carbon catalyst to afford model compounds, **1**, **2**, **3**, or **4**, in quantitative yields.

The Iron Complexes of the Model Compounds. Fe(II) complexes of the model compounds **1**—**4** in Tris-HCl (pH 7.2) showed the characteristic UV-vis absorption under an anaerobic conditions with the absorption maximum at 471—472 nm, which is similar to that of the BLM–Fe(II) complex (Table 1).[53,54] The Fe(II) complexes were easily oxidized to form to corresponding stable Fe(III) complexes (absorption at 384—391 nm) in the presence of O_2 (Fig. 2). However, the Fe(II) complex of model compound **5**, which has no steric factor, was very unstable under the same conditions,

Table 1. Electron Spectral Data of Fe(II) and Fe(III) Complexes

Ligand	λ_{max}/nm (ε)		
	Fe(II) complex	Fe(III) complex	Fe(III)–DTT adduct
BLM	476 (380)[a]	384 (1900)[a]	589 (673)
1	471 (557)	386 (2152)	613 (1159)
2	471 (546)	384 (2207)	615 (1199)
3	472 (606)	387 (1935)	614 (1405)
4	472 (661)	391 (2052)	601 (1248)

In Tris-HCl buffer (pH 7.2); ε in $mol^{-1}\,dm^{3}cm^{-1}$. a) Data from Ref. 54.

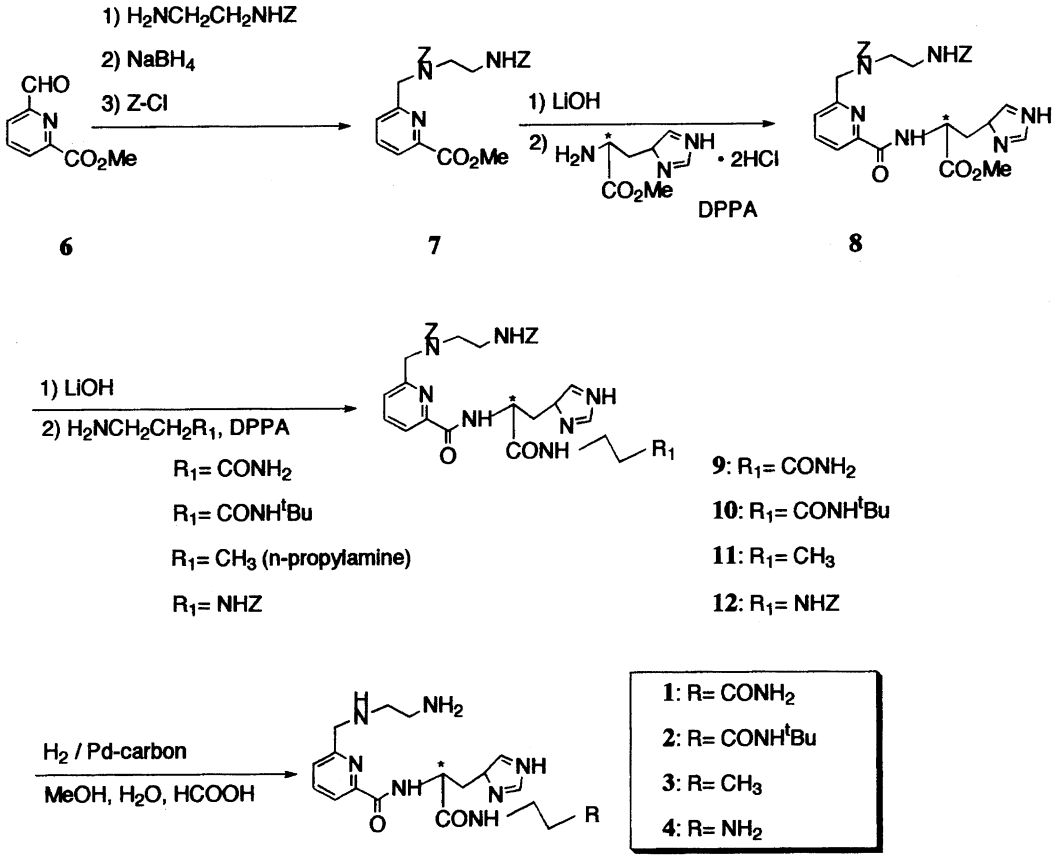

Scheme 1. Synthesis of BLM model compounds.

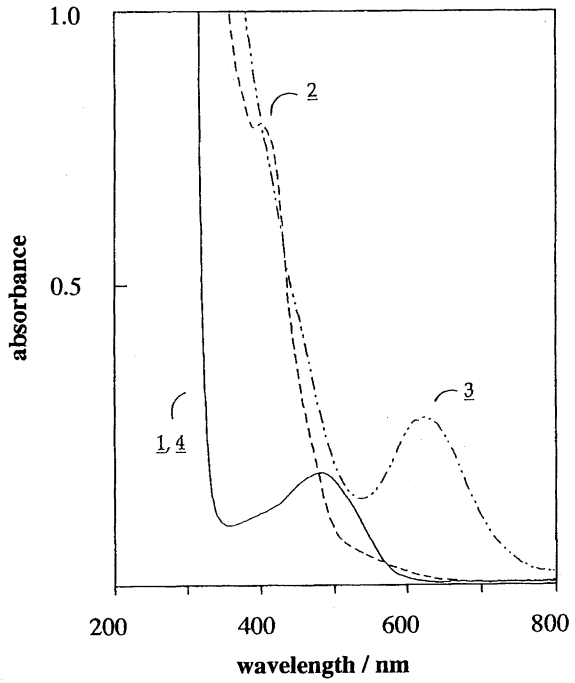

Fig. 2. Reversible redox reaction of **1**–Fe(II) complex. The concentration of Fe(II) complex was 0.5 mM in 50 mM Tris-HCl (pH 7.2), and the spectra were taken under the following condition; 1 (—), under Ar (λ_{max}=471 nm); 2 (– – –), O_2 bubbling to the sample 1 (λ_{max}=386 nm); 3 (– ·· –), the addition of DTT (1.0 mM) to the sample 2; 4 (—), 60 min after the addition of DTT to the sample 2.

and the precipitation of iron(III) hydroxide was observed.[30] A bulky group, such as a *t*-butyl group,[15,21,22,25] a long alkyl group,[30] or a saccharide group[55] has been reported to enhance the stability of the Fe(III) complex, inhibiting the liberation of the Fe(III) ion from the complex. The present studies demonstrate that a simple 2-carbamoylethyl, propyl, or 2-aminoethyl group, was also effective in enhancing the stability of the Fe(III) complex of the BLM model compound.

The possible coordination of the carbamide group of **1** to the metal ion was investigated by IR spectroscopy.[42,51] IR bands due to ν_{CO} were observed at 1557, 1521, and 1650 cm^{-1} for the **1**–Fe(II) complex, and 1644, 1651, and 1673 cm^{-1} for compound **1**. The ligation of compound **1** to Fe(II) is characterized by a shift of ν_{CO} of the first secondary amide between the pyridyl and imidazolyl moiety from 1673 cm^{-1} in the free ligand to 1557 cm^{-1} in the complex. A lower wavelength shift of ν_{CO} of this secondary amide by coordination to the metal ion was also observed in the metal complex of **5**.[51] Coordination of the terminal carbamide group to the Fe(II) is likely indicated by a shift of its ν_{CO} from 1644 cm^{-1} in the free state to 1521 cm^{-1} in the complex. On the other hand, ν_{CO} due to the second secondary amide, which is incapable of coordination to the metal ion, showed very small shift of the IR band from a free to a complexed state. Although the IR data suggest a coordination of the carbamide group of **1** to the chelated Fe(II) ion, an X-ray crystal analysis is required for the confirmation of the structure. An effort to crystallize the **1**–Fe(II) or the corresponding **1**–Co(III) complex for an X-ray analysis has so far been unsuccessful.

The addition of DTT to the Fe(III) complexes of **1**—**4** resulted in the formation of a DTT adduct of the Fe(III) complexes, which showed characteristic absorption spectra at around 600 nm, and then gradually regenerated to the initial Fe(II) complex by the reduction of the Fe(III) complexes with DTT, as shown in Fig. 2. The formation of stable Fe(III) complexes of **1**—**4** and the cycle of the reversible redox reaction by DTT, which is a characteristic of the Fe(III) complex of BLM, was also confirmed by EPR. A decrease in the *g*-value splitting of the Fe(III) complexes upon the addition of DTT implies an axial coordination of the thiol ligand to the Fe(III) complexes. Table 2 gives the EPR parameters of the Fe(III) complexes and their DTT adducts. The EPR parameters are also very close to those of the BLM–Fe(III) complex.[54,56]

Protonation Constants, pK_a, of the Model Ligands. The protonation constants of the BLM model compounds were determined by potentiometeric titration at 25 °C in the presence of 0.1 M $NaClO_4$. Compounds **1**—**3**, obtained as *tris*-perchlorate salts and purified by crystallization, were used for the titration. The titrated data were analyzed by a computer program, SUPERQUAD.[52] The log values of the protonation constant (pK_1, pK_2, and pK_3) of the model compounds are given in Table 3 along with those of BLM[57] and the simplest model compounds **5**.[50] The protonated species of **1** are illustrated in Scheme 2. A model compound bearing a terminal carbamide group, **1**, showed lower pK_1, pK_2, and pK_3 values than any other model compounds, although the values were higher than those of BLM. The simplest model compound, **5** or the model compound **3**, bearing a propyl group, exhibited rather higher pK values. The smaller pK values of model compound **1** are likely to be derived from an electron-withdrawing effect of the carbamide group. The low pK_1 value of the terminal α-amino group of the model

Table 2. EPR Parameters of Fe(III) Complexes

Ligand	Fe(III) complex [Fe(III)–DTT adduct][a]		
	g_1	g_2	g_3
BLM	2.431[b] [2.289]	2.185[b] [2.161]	1.893[b] [1.918]
1	2.355 [2.253]	2.183 [2.171]	1.882 [1.940]
2	2.354 [2.246]	2.186 [2.172]	1.887 [1.941]
3	2.354 [2.246]	2.179 [2.168]	1.880 [1.935]
4	2.364 [2.258]	2.183 [2.175]	1.886 [1.944]

a) EPR parameters for the Fe(III)–DTT adduct complex are shown in the bracket. b) Data from Ref. 54.

Table 3. Protonation Constants of Model Compounds and BLM

Compound	pK_1 (–NH–)	pK_2 (–Im)	pK_3 (–NH_2)
BLM	2.9[a]	5.0[a]	7.7[a]
1	5.3	6.1	8.7
2	5.3	6.2	8.9
3	5.9	6.5	9.3
5	5.6[b]	7.3[b]	9.8[b]

At 25 °C and I=0.1 ($NaClO_4$). a) Data from Ref. 58. b) Data from Ref. 50.

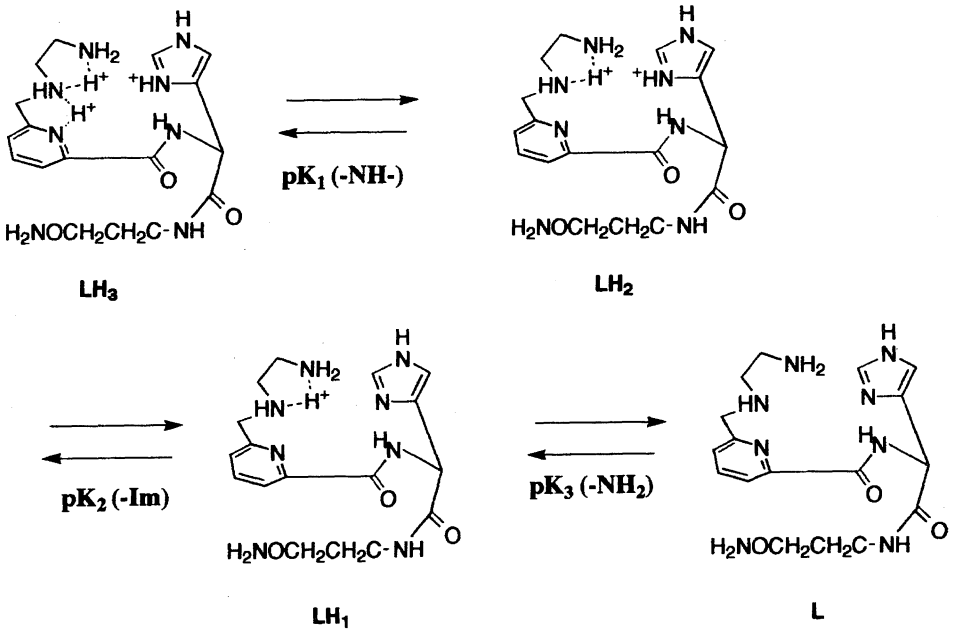

Scheme 2. Protonated species of BLM model compound **1**.

compound assists the axial α-amino nitrogen coordination over wide pH ranges. Kimura and co-workers showed that carbamide of the β-aminoalanyl portion in BLM works to lower the overall basicity of the amino donors,[50] which enables the amino groups to bind with the metal ion over the competing protons. Our results demonstrate that the terminal carbamide group in compound **1** also lowers the pK values of the amino donors of the ligand and enhances complex formation with the metal ion over wide pH ranges.

Oxygen Activation of Iron Complexes of the Model Compounds. The oxygen activation of the Fe(II) complexes of the model compounds in a one-cycle oxidation process was assessed by an EPR spin-trapping experiment using *N*-*t*-butyl-α-phenylnitron (PBN) as a spin-trapping agent. The EPR parameters, triplet of a doublet with a g factor of g_H=2.01 and a_H=15.0 G, were identical with those of the hydroxyl-PBN spin adduct.[56,58] The spin concentration of the hydroxyl radical generated from the Fe(II) complexes of model compounds, **1**, **2**, **3**, and **4** with molecular oxygen were estimated to be 74, 69, 43, and 31%, respectively, of that of the BLM standard. It is noteworthy that model compound **1**, bearing a simple carbamide group which can coordinate to the iron ion as a sixth ligand, showed a higher oxygen activation ability compared to that of **2** bearing a bulky *t*-butyl group. On the other hand, a model compound bearing a terminal amino group, which may coordinate to the Fe(II) ion as a sixth ligand, exhibited a low oxygen activation ability compared to other model compounds. The reason for the higher oxygen activation ability of the iron complex of **1**, compared to **4**, is not clear; however, we believe that the electron-withdrawing effect of the carbamide group lowers the pK values of the amino donors of the model compounds, thus enhancing the complexing ability and, thus, the oxygen activation ability. The carbamoyl-sugar residue of BLM has been suggested to provide stabilization of the activated BLM by a hydrogen-bonding interaction with the dioxygen moiety of the iron-complex of BLM.[43] Likewise, the carbamide group in the iron complex of **1** may enhance the stability of the coordinated oxygen or oxygenated species of the iron complex of **1** by a hydrogen-bonding interaction between the coordinated oxygen or oxygenated species with the carbamide group. Further, Boger et al. have shown that the acetamide side chain at the α-position of the pyrimidine ring of BLM significantly enhances the DNA cleavage efficiency, although it is not involved in metal chelation.[59] The amide group in the simple model compound **1** could play the role of the same group in the dissacharide moiety or at the α-position of the pyrimidine ring of BLM in attenuating the oxygen activation ability of the Fe(II) complex.

Kinetic Studies of Redox Reactions of the Iron Complexes of the BLM Model Compounds. We have studied the kinetics of the oxidation and reduction processes of the iron complexes of BLM and model compounds. Very few studies have been reported on the kinetics of the oxygenation and subsequent oxidation of the BLM–Fe(II) complex.[9] Overall, the oxygen activation of the Fe(II) complexes depends on the turnover of the cycle of the redox reactions which involve oxidation of the Fe(II) complexes to the Fe(III) complexes and regeneration of the Fe(II) complexes by reduction of the oxidized Fe(III) complexes. The reaction of the Fe(II) complexes of BLM model compounds with oxygen took place within a second at 20 °C to form the corresponding Fe(III) complexes, in accordance with the change in the color of the solution from pink to orange. The reaction is considered to proceed via the following pathway from the Fe(II) complex: (1) formation of an oxygenated intermediate, (2) activation of this oxygenated intermediate to the transient activated Fe(III) complex, and (3) conversion of the activated Fe(III) complex to the stable Fe(III) complex.[9,10]

$$\textbf{1}\text{–Fe(II)} + O_2 \xrightarrow{(1)} \textbf{1}\text{–Fe(II)–}O_2 \text{ or } 1\text{–Fe(III)–}O_2^-$$
$$\xrightarrow{(2)} \text{transient activated } \textbf{1}\text{–Fe(III)} \xrightarrow{(3)} \text{stable } \textbf{1}\text{–Fe(III)}$$

Since the electronic spectrum of the transient activated species was very close to that of the stable Fe(III) species, we could not differentiate these two by the spectrophotometric method. However, the two species showed distinct EPR spectra. The transient activated species was detected in a small amount along with the stable Fe(III) species by EPR 5 s after a reaction of the Fe(II) complex with O_2 at 20 °C and subsequent freezing at 77 K. However, only the stable Fe(III) species was observed 20 s after the reaction with O_2. We have studied the reaction kinetics of the oxygenation of the Fe(II) complexes of BLM model compounds and the subsequent formation of the Fe(III) species by a stopped-flow apparatus monitored at the 386 nm absorption change. In the presence of a large excess amount of O_2 over the Fe(II) complexes, the step (1) reaction is considered to be a pseudo first-order reaction. The spectral change of the **1**–Fe(II) complex in the presence of a 20-fold excess of O_2 is shown in Fig. 3. The first, rapid kinetic event corresponds to step (1) and the subsequent slower process to step (2). Plots of log of the absorption change against time at initial times are linear, indicating a first-order dependence of the reaction rate on the Fe(II) complex concentration. The rate of the reaction is linear against the O_2 concentration, as shown in Fig. 4. Thus, reaction step (1) is second order, with a rate constant of $k=1.1\times10^4$ mol^{-1}dm^{-3} s^{-1} at 20 °C; the first-order dependence on O_2 and the first-order dependence on the Fe(II) complex. The reaction rates of step (1) for the Fe(III) complexes of model ligands **1**—**4** are listed in Table 4, along with that for the Fe(II)–BLM complex at 20 °C, which has been estimated from the published results.[9] In reaction step (2), the product of the step (1) reaction, the oxygenated Fe(II) complex, converted to the Fe(III) species with first-order kinetics of $k=0.62$ s^{-1} at 20 °C, which was independent of the oxygen concentration. The intermediate Fe(III) species converted to the stable Fe(III) species, although these two are spectrophotometrically indistinguishable. The rate constant of step (2) for the Fe(II) complexes of the BLM model compounds are also given in Table 4. The rates of steps (1) and (2) for the Fe(II) complexes of the simplified BLM model compounds resemble to those for the BLM–Fe(II) complex, although the rate of step (1) for the Fe(II)–BLM complex was shown to be 1.8—2.8 times higher than that for the Fe(II) complexes of the model compounds. On the other hand, step (2) for the BLM complex proceeded 1.6—2.0 times slower than that for the complexes of the simplified BLM model compounds. The rate of step (1) for the **2**–Fe(II) complex was slightly lower than that for the **1**–Fe(II), probably due to the hydrophobic steric hindrance of the bulky *t*-butyl group of **2**. The terminal primary amino group in the **4**–Fe(III) complex also retarded the step (1) reaction, since this amino group can coordinate to the Fe(II) complex strongly as a sixth ligand, inhibiting the ligand substitution with O_2. The rate-constant step (2) is namely the same for the Fe(II) complexes of model compounds **1**—**4**.

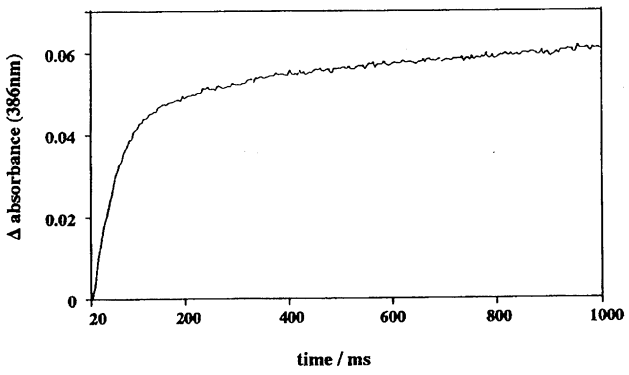

Fig. 3. Spectral change of reaction of **1**–Fe(II) complex with O_2. Reaction of **1**–Fe(II) complex (0.10 mM) with O_2 (2.0 mM) in 10 mM Tris-HCl (pH 7.2) at 20 °C was monitored by absorbance at 386 nm.

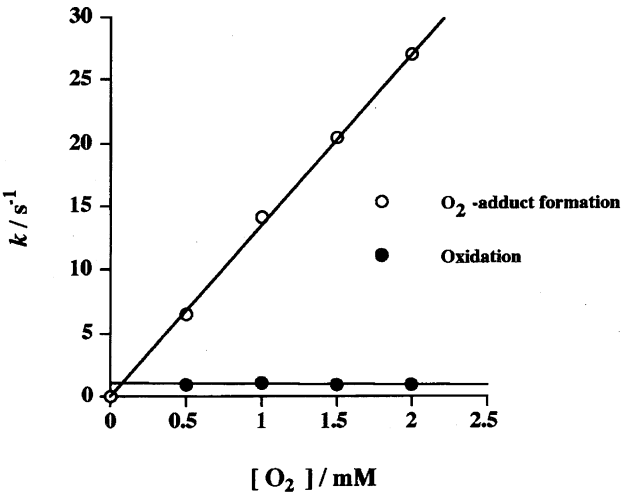

Fig. 4. Dependence of the ratio of O_2-adduct formation and subsequent oxidation of **1**–Fe(II) complex on O_2 concentration. The plots were constructed from the spectal change of the **1**–Fe(II) complex depicted in Fig. 3.

Table 4. Rate Constants of Oxygenation and Subsequent Oxidation for Fe(II) Complexes with O_2

Ligand	k_{add}/mol^{-1} dm^3 s^{-1}	k_{oxi}/s^{-1}
BLM	1.8×10^4 a)	3.3×10^{-1} a)
1	1.1×10^4	6.2×10^{-1}
2	8.6×10^3	6.6×10^{-1}
3	1.0×10^4	5.3×10^{-1}
4	6.5×10^3	6.6×10^{-1}

k_{add}: second order rate constant; first order dependence on O_2 and first order dependence on the Fe(II) complex. k_{oxi}: first order rate constant; first order dependence on the product of the step (1). a) Data from Ref. 9.

Next, we studied the reaction kinetics of the reduction of the Fe(III) complexes of BLM or model compounds with a reducing agent, dithiothreitol (DTT). The DTT adduct formation of the **1**–Fe(III) complex and the subsequent reduction, shown in the following scheme, was monitored by the change of absorption at 613 nm, which is ascribed to that of the DTT adduct of the Fe(III) complex (Fig. 5).

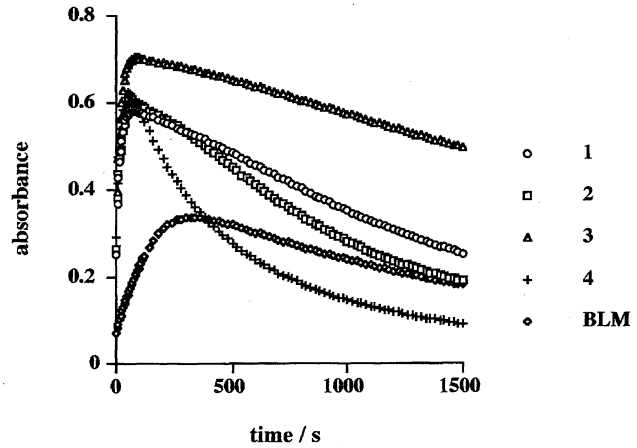

Fig. 5. Absorption change of reduction of the Fe(III)-complexes with DTT. Reaction of the Fe(III)-complexes of the model compounds or BLM with DTT (1.0 mM) in Tris–HCl (pH 7.2) at 20 °C monitored by absorbance at the λ_{max} of the DTT adduct of the Fe(III) complex; **1**: 613 nm, **2**: 615 nm, **3**: 614 nm, **4**: 601 nm, BLM: 589 nm.

$$\text{stable } \mathbf{1}\text{–Fe(III)} + \text{DTT} \xrightarrow[\text{(Adduct formation)}]{} \mathbf{1}\text{–Fe(III)–DTT} \xrightarrow[\text{(Reduction)}]{} \mathbf{1}\text{–Fe(II)}$$

This reaction process was also observed based on a change of the EPR spectroscopy. The linear relationship of plots of $1/(a-b)\ln\{b(a-x)/a(b-x)\}$ vs. time at the initial reaction periods, where a is the initial concentration of DTT, b is the initial concentration of the Fe(III) complex, and x is the concentration of the adduct, denotes that the first reaction step proceeds depending on the second order; the first-order dependence on DTT and the first-order dependence on the Fe(III) complex (Fig. 6a). The reaction rates of the adduct formation obtained from the slope of the plots are listed in Table 5. The adduct formation of the Fe(III) complexes of model compounds **1**—**4** were 6—8 times higher than that of BLM, probably because the hydrophilic bulky carbamoyl-attached disaccharide moiety of BLM suppresses the introduction of the bulky DTT.

The reduction of the Fe(III) complexes via the DTT adduct, the second reaction step, was monitored based on the disappearance of absorption at 613 nm. Plots of the log of the spectral change against the time showed a linear relationship, which demonstrates that this process is first-order

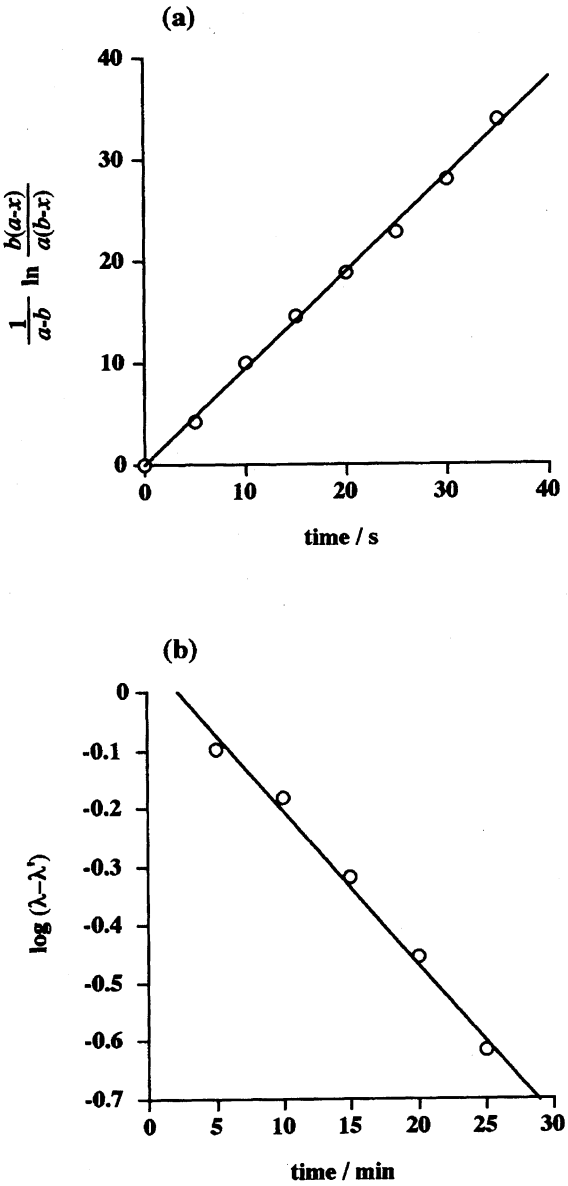

Fig. 6. Rate of kinetic event observed for the reaction of **1**–Fe(III) complex with DTT.
(a) Second order reaction of the **1**–Fe(III) complex with DTT. (b) Guggenheim plot of reduction of the **1**–Fe(III)–DTT adduct. The plots were constructed from the spectal change of the **1**–Fe(III) complex depicted in Fig. 5.

Table 5. Rate Constants of DTT–Adduct Formation and Subsequent Reduction for Fe(III) Complex with DTT

Ligand	k_{add}/mol^{-1} dm^{-3} s^{-1}	k_{red}/s^{-1}
BLM	1.4×10^{-2}	1.9×10^{-2}
1	9.5×10^{-2}	2.6×10^{-2}
2	8.5×10^{-2}	3.4×10^{-2}
3	8.8×10^{-2}	9.9×10^{-2}
4	1.1×10^{-1}	6.7×10^{-2}

k_{add}: second order rate constant; first order dependence on DTT and first order dependence on the Fe(III) complex. k_{red}: first order rate constant: first order dependence on DTT–adduct of the Fe(III) complex.

dependent on the adduct, as shown in Fig. 6b. The rate constants of the reduction are also listed in Table 5. This is the first kinetic data of the reduction of the BLM–Fe(III) complex. It is noteworthy that the rates of the adduct formation and the subsequent reduction of the Fe(III) complex of BLM or model compounds are more than ten-times lower than those of the oxygenation and the subsequent oxidation of the corresponding Fe(II) complexes. The results demonstrate that regeneration of the Fe(II) species from the stable oxidized Fe(III) complex with a reducing agent takes place rather slowly, indicating the low turnover of the formation of the reactive Fe(II) complexes of BLM, which is responsible

for the DNA cleavage, since the Fe(III) complex of BLM degrades slowly along with the precipitation of iron(III) hydroxide. Contrary to the results of the oxygenation and the subsequent oxidation, the rates of the DTT adduct formation and the subsequent reduction are slower for the Fe(III)–BLM complex compared to the Fe(III) complexes of the simple model compounds. Among the BLM and the model compounds, **4**, which bears a primary amino group around the sixth coordination site, exhibited the highest rates for adduct formation and reduction, probably because of the electron-donating character of the amino group.

In conclusion, we confirmed that the substituent group of the BLM model complex around the sixth coordination site has a profound effect on the oxygen-activation ability and the rates of the redox reaction of the iron complex of the BLM model compounds. Among the model compounds, **1**, which has a simple carbamide group, exhibited the highest oxygen activation ability. The carbamide group of **1** may have a similar role to the same group in BLM in the oxygenation process of the Fe(II) complex. Further, we confirmed that the reduction of the Fe(III) complexes of BLM and model compounds with a reducing agent proceeds far more slowly compared to the oxidation of the corresponding Fe(II) complexes with O_2.

References

1) H. Umezawa, K. Maeda, Y. Takeuchi, and Y. Okami, *J. Antibiot., Ser. A.*, **19**, 200 (1966).

2) R. H. Blum, S. K. Carter, and K. A. Agre, *Cancer*, **31**, 903 (1973).

3) H. Umezawa, in "Bleomycin: Chemical, Biochemical, and Biological Aspects," ed by S. M. Hecht, Springer-Verlag, New York (1979), p. 24.

4) Y. Sugiura, T. Takita, and H. Umezawa, in "Metal Ions in Biological Systems," ed by H. Sigel, Dekker, New York (1985), Vol. 19, p. 81.

5) S. M. Hecht, *Acc. Chem. Res.*, **19**, 383 (1986).

6) J. Stubbe and J. W. Kozarich, *Chem. Rev.*, **87**, 1107 (1987).

7) S. A. Kane and S. M. Hecht, *Prog. Nucleic Acid Res. Mol. Biol.*, **49**, 313 (1994).

8) J. Stubbe, J. W. Kozarich, W. Wu, and D. E. Vanderwall, *Acc. Chem. Res.*, **29**, 322 (1996).

9) R. M. Burger, S. B. Horwitz, J. Peisach, and J. B. Wittenberg, *J. Biol. Chem.*, **254**, 12299 (1979).

10) R. M. Burger, J. Peisach, and S. B. Horwitz, *J. Biol. Chem.*, **256**, 11636 (1981).

11) R. M. Burger, T. A. Kent, S. B. Horwitz, E. Munck, and J. Peisach, *J. Biol. Chem.*, **258**, 1559 (1983).

12) J. W. Sam, X. J. Tang, and J. Peisach, *J. Am. Chem. Soc.*, **116**, 5250 (1994).

13) R. M. Burger, G. Tian, and K. Drlica, *J. Am. Chem. Soc.*, **117**, 1167 (1995).

14) A. L. Feig and S. J. Lippard, *Chem. Rev.*, **94**, 759 (1994).

15) M. Ohno and M. Otsuka, in "Recent Prog. Chem. Synth. Antibiotics," ed by G. Lukacs and M. Ohno, Springer-Verlag, New York (1990), p. 387.

16) M. Otsuka, M. Yoshida, S. Kobayashi, M. Ohno, Y. Sugiura, T. Takita, and H. Umezawa, *J. Am. Chem. Soc.*, **103**, 6986 (1981).

17) J.-P. Henichart, R. Houssin, J.-L. Bernier, and J.-P. Catteau, *J. Chem. Soc., Chem. Commun.*, **1982**, 1295.

18) J.-P. Henichart, J. L. Bernier, R. Houssin, M. Lohez, A. Kenani, and J. P. Catteau, *Biochem. Biophys. Res. Commun.*, **126**, 1036 (1985).

19) R. E. Kilkuskie, H. Suguna, B. Yellin, N. Murugesan, and S. M. Hecht, *J. Am. Chem. Soc.*, **107**, 260 (1985).

20) A. Kittaka, Y. Sugano, M. Otsuka, M. Ohno, Y. Sugiura, and H. Umezawa, *Tetrahedron Lett.*, **27**, 3631 (1986).

21) Y. Sugano, A. Kittaka, M. Otsuka, M. Ohno, Y. Sugiura, and H. Umezawa, *Tetrahedron Lett.*, **27**, 3635 (1986).

22) M. Otsuka, A. Kittaka, M. Ohno, T. Suzuki, J. Kuwahara, Y. Sugiura, and H. Umezawa, *Tetrahedron Lett.*, **27**, 3639 (1986).

23) A. Kenani, M. Lohez, R. Houssin, N. Helbecque, J. Bernier, P. Lemay, and J. P. Henichart, *Anticancer Drug Design*, **2**, 47 (1987).

24) S. J. Brown and P. K. Mascharak, *J. Am. Chem. Soc.*, **110**, 1996 (1988).

25) A. Kittaka, Y. Sugano, M. Otsuka, and M. Ohno, *Tetrahedron*, **44**, 2811 (1988).

26) T. J. Lomis, J. F. Siuda, and R. E. Shepherd, *J. Chem. Soc., Chem. Commun.*, **1988**, 290.

27) M. Cristini, P. Scrimin, and U. Tonellato, *Tetrahedron Lett.*, **30**, 2987 (1989).

28) T. J. Lomis, M. G. Elliott, S. Siddiqui, M. Moyer, R. R. Koepsel, and R. E. Shepherd, *Inorg. Chem.*, **28**, 2369 (1989).

29) A. Suga, T. Sugiyama, M. Otsuka, M. Ohno, Y. Sugiura, and K. Maeda, *Tetrahedron*, **47**, 1191 (1991).

30) K. Shinozuka, H. Morishita, T. Yamazaki, Y. Sugiura, and H. Sawai, *Tetrahedron Lett.*, **32**, 6869 (1991).

31) D. L. Boger, R. F. Menezes, Q. Dang, and W. Yang, *Bioorg. Med. Chem. Lett.*, **2**, 261 (1992).

32) J. D. Tan, S. E. Hudson, S. J. Brown, M. M. Olmstead, and P. K. Mascharak, *J. Am. Chem. Soc.*, **114**, 3841 (1992).

33) D. L. Boger, R. F. Menezes, and Q. Dang, *J. Org. Chem.*, **57**, 4333 (1992).

34) R. J. Guajardo, J. D. Tan, and P. K. Mascharak, *Inorg. Chem.*, **33**, 2838 (1994).

35) R. J. Guajardo, S. E. Hudson, S. J. Brown, and P. K. Mascharak, *J. Am. Chem. Soc.*, **115**, 7971 (1993).

36) L. Huang, R. Morgan, and J. W. Lown, *Bioorg. Med. Chem. Lett.*, **3**, 1751 (1993).

37) E. Farinas, J. D. Tan, N. Baidya, and P. K. Mascharak, *J. Am. Chem. Soc.*, **115**, 2996 (1993).

38) D. L. Boger, T. Honda, R. F. Menezes, S. L. Colletti, Q. Dang, and W. Yang, *J. Am. Chem. Soc.*, **116**, 82 (1994).

39) T. Sugiyama, M. Ohno, M. Shibasaki, M. Otsuka, Y. Sugiura, S. Kobayashi, and K. Maeda, *Heterocycles*, **37**, 275 (1994).

40) J. Kohda, K. Shinozuka, and H. Sawai, *Tetrahedron Lett.*, **36**, 5575 (1995).

41) L. Huang, J. C. Quada, Jr., and J. W. Lown, *Bioconjugate Chem.*, **6**, 21 (1995).

42) R. J. Guanjardo, F. Chavez, E. T. Farinas, and P. K. Mascharak, *J. Am. Chem. Soc.*, **117**, 3883 (1995).

43) A. Kenani, C. Bailly, N. Helbecque, J.-P. Catteau, R. Houssin, J.-L. Bernier, and J.-P. Henichart, *Biochem. J.*, **253**, 497 (1988).

44) L. H. DeReimer, C. F. Meares, D. A. Goodwin, and C. I. Diamanti, *J. Med. Chem.*, **22**, 1019 (1979).

45) N. J. Oppenheimer, L. O. Rodriguez, and S. M. Hecht, *Proc. Natl. Acad. Sci. U. S. A.*, **76**, 5616 (1979).

46) N. J. Oppenheimer, C. Chang, L.-H. Chang, G. Ehrenfeld, L. O. Rodriguez, and S. M. Hecht, *J. Biol. Chem.*, **257**, 1606 (1982).

47) H. Sugiyama, R. E. Kilkuskie, L.-H. Chang, L.-T. Ma, S. M. Hecht, G. A. van der Marel, and J. H. van Boom, *J. Am. Chem. Soc.*, **108**, 3852 (1986).
48) D. L. Boger, S. Teramoto, and J. Zhou, *J. Am. Chem. Soc.*, **117**, 7344 (1995).
49) T. Arai, K. Shinozuka, and H. Sawai, *Bioorg. Med. Chem. Lett.*, **7**, 15 (1997).
50) E. Kimura, H. Kurosaki, Y. Kurogi, M. Shionoya, and M. Shiro, *Inorg. Chem.*, **31**, 4314 (1992).
51) W. Mathes, W. Sauermilch, and T. Klein, *Chem. Ber.*, **86**, 584 (1953).
52) P. Gans, A. Sabatini, and A. Vacca, *J. Chem. Soc., Dalton Trans.*, **1985**, 1195.
53) Y. Sugiura, T. Suzuki, M. Otsuka, S. Kobayashi, M. Ohno, T. Takita, and H. Umezawa, *J. Biol. Chem.*, **258**, 1328 (1983).
54) Y. Sugiura, T. Suzuki, H. Kawabe, H. Tanaka, and K. Watanabe, *Biochem. Biophys. Acta*, **716**, 38 (1982).
55) A. Kenani, C. Bailly, N. Helbecque, R. Houssin, J.-L. Bernier, and J.-P. Henichart, *Eur. J. Med. Chem.*, **24**, 371 (1989).
56) Y. Sugiura, *J. Am. Chem. Soc.*, **102**, 5208 (1980).
57) Y. Sugiura, K. Ishizu, and K. Miyoshi, *J. Antibiot.*, **32**, 453 (1979).
58) Y. Sugiura and T. Kikuchi, *J. Antibiot.*, **31**, 1310 (1978).
59) D. L. Boger, T. Honda, R. F. Menezes, S. L. Colletti, Q. Dang, and W. Yang, *J. Am. Chem. Soc.*, **116**, 82 (1994).